Numerical investigation of compressibility effects on friction factor in rectangular microchannels

Numerical investigation of compressibility effects on friction factor in rectangular microchannels

P. Vocale[a*], D. Rehman[b], G. L. Morini[b]

[a] Department of Engineering and Architecture, University of Parma, Parco Area delle Scienze 181/A - 43124 Parma, Italy

[b] DIN – Alma Mater Studiorum Università di Bologna, Laboratorio di Microfluidica, Via Lazzaretto 15, Bologna 40131, Italy

* Corresponding author.

E-mail addresses
pamela.vocale@unipr.it
danish.rehman88@gmail.com
gianlucamorini3@unibo.it

Abstract. In the present paper, the gas compressibility effect on friction factor in rectangular microchannels is numerically investigated. First of all, the numerical model adopted in the present study has been validated against experimental data obtained by testing rectangular microchannels with a hydraulic diameter of 295 μm. The numerical model is used for evaluating in correspondence of which value of the Reynolds number the compressibility effects on the friction factor become significant by analysing the role of both hydraulic diameter and aspect ratio of the microchannel. To this aim, three values of the hydraulic diameter (100, 295 and 500 μm) and five different aspect ratios (from 0.25 to 1) has been investigated. The numerical results highlight that compressibility effects become stronger and stronger by reducing the hydraulic diameter and they lead to an increase of the average friction factor. For smaller microchannels the Reynolds numbers in correspondence of which the compressibility effects become significant tend to be reduced and already in laminar regime the compressibility gas nature cannot be ignored when friction factors have to be accurately determined. Moreover, for narrow microchannels (low aspect ratio) compressibility effects become important for higher values of the Reynolds number than those observed for nearly squared microchannels.

Keywords: Compressibility effects; Entrance effects; Friction factor; Rectangular microchannels; Microfluidics.

1. Introduction

During the last decades, several works have been addressed to the analysis of pressure drops in microchannels with inner dimensions lower than 1 mm because the reduction of the inner dimensions of the channels can introduce scaling effects that must be taken into account for a correct evaluation of the pressure drop [1]. As an example, when the inner diameter of the channel is reduced, for a fixed value of the Reynolds number an increase in the average velocity is obtained. The increase in the average velocity can be very strong for gas flows through microchannels where velocity values larger than 100 m/s can be reached at low Reynolds numbers. In this case the pressure drop can be affected by compressibility effects for Reynolds numbers lower than 2000 (laminar regime) while for conventional tubes these effects tend to become important only in turbulent regime (large Reynolds numbers).

The effects of compressibility on the fluid-dynamic behaviour of gas flows in microchannels with circular cross-section have been studied since a long time. Guo et al. [2-4] analytically and numerically studied the compressibility effects in microtubes. The outcomes of their works pointed out that the flow compressibility made the fluid velocity profiles flatter resulting in higher friction factors than those of conventional sized tubes. Morini et al. [5] experimentally investigated commercial stainless steel long microtubes with the hydraulic diameter in the range 762-127 μm. Three different methods were employed to calculate the friction factor with varying Reynolds number and recommended that for the long microtubes the friction factor can better be calculated using isothermal flow assumption [6]. It was found that compressibility effects become quite significant for higher Reynolds numbers or smaller hydraulic diameters due to increased pressure drop which causes strong density variations of the gas along the length of the microtube.

Morini et al. [7] also performed experimental investigations of compressibility effect on the average friction factor for nitrogen flow in microtubes with diameters in the range of 100–300 μm. Their results confirmed that in the laminar regime the agreement with the conventional theory was very good, especially for long microtubes. On the other hand, for microchannels characterized by a length lower than 0.05 m, the friction factor deviated from the conventional incompressible flow theory when the Reynolds number became higher than 1000.

Similar trends were found by Celata et al. [8] who carried out experimental study of the compressibility and rarefaction effects in fused silica microtubes having a diameter in the range 30 - 254 μm, and for Reyndols number lower than 600. Their outcomes showed that friction factor values were remarkably close to the theoretical predictions and hence no effect of compressibility could be observed if the experimental uncertainty was catered for.

Celata et al. [9] also performed experimental investigations of the compressibility effects in microtubes characterized by diameters ranging between 30 μm and 500 μm. Their findings revealed that, due to the acceleration associated with compressibility effects, a deviation from the Poiseuille law occurred in microtubes with diameters lower than 100 μm for Reynolds numbers higher than 1300.
Compressibility effects in microtubes were also experimentally investigated by Tang e t al. [10] who tested microtubes with diameters ranging from 50 to 300 μm in laminar flow regime. They observed an increase of the friction factor with respect the values of the conventional incompressible flow theory. Moreover, they developed a correlation that enabled to evaluate the increase in the friction factor due to the compressibility effects depending on the Mach number.
The same outcomes were highlighted by Vijayalakshmi et al. [11] and by Hong et al. [12] who carried out experimental studies of gas compressibility in microtubes characterized by diameters ranging from 60 to 211μm [11] and from 500 down to 150 μm [12].
On the other hand, there are only few studies of gas compressibility effects in microchannels characterized by non-circular cross-sections. Wu and Little [13] investigated the friction resistance characteristics of a gas flow in very fine channels (i.e. channels characterized by hydraulic diameters ranging between 45 μm and 83 μm) used for microrefrigerators. Their results revealed that the friction factor in small channels is affected by many factors, such as the dimensions of the channel, the methods of etching and the surface treatments. In particular, they found that even in the laminar zone, the values of the friction factor were affected by roughness.
Asako et al. [14,15] numerically investigated the compressibility effects in parallel plates. In particular, by considering both adiabatic and isothermal wall conditions, they found that for Mach number at the channel outlet higher than 0.4 the values of the Poiseuille number (i.e. product of Fanning friction factor and the Reynolds number) differed from the theoretical values. They also proposed correlations for evaluating the friction factor, which can be used for Reynolds and Mach numbers lower than 500 and 0.4, respectively.
The fluid behaviour of compressible flows in parallel plates was also numerically investigated by Cavazzuti et al. [16] who developed a new correlation for evaluating the friction factor for compressible flows in parallel plates that can be used for Reynolds and Mach numbers lower than 2300 and 1, respectively
Hong et al. [17] experimentally analysed rectangular microchannels by measuring the local pressure of the gas flow inside the channels in the axial direction. Hydraulic diameters ranged between 69 μm and 148 μm whereas the aspect ratio of the microchannels was in the range 0.036-0.078. The experiments were carried out in laminar, transitional and turbulent flow regimes. They defined a semi-local Fanning friction factor evaluated by using the measured pressure at two consecutive pressure ports along the channel. They found that in laminar flow regime the values of the semi-local friction factor were slightly higher than macro scale prediction. Furthermore, they proposed a correlation that enabled to evaluate the friction factor as a function of the Mach number, for Reynolds numbers lower than 600.
Rectangular microchannels were also experimentally and numerically investigated by Rehman et al. [18]. In particular, by considering three microducts characterized by different hydraulic diameters and aspect ratios, they evaluated the influence of the minor loss coefficients on the average friction factor.
As can be seen from the literature survey, there seem to be few studies on the analysis of fluid-dynamic behaviour of compressible flows in rectangular microchannels, although the majority of micro heat sinks and micro heat exchangers are based on rectangular microchannels due to the typical constraints linked to the employed microfabrication techniques and to the characteristics of the selected solid substrate [19]. As an example, when a heat sink is obtained using a silicon <110> substrate and the microchannels are made by chemical etching the rectangular cross section of the obtained microchannels is imposed by the crystallographic morphology of the <110> silicon [20]. If a plastic/metallic substrate is used, micro-milling techniques allow to make rectangular microchannels in a simple and chip way and for this reason this cross section geometry is very popular in microfluidics [21].
If microchannels have a rectangular cross section, the aspect ratio (defined as the ratio between the height and width of the channel) plays a role on the flow which cannot be studied by using calculations

made for rounded tubes. Shallow, deep or squared channels exhibit a very different fluid-dynamic behaviour in terms of friction factor for the same hydraulic diameter. The effect of the aspect ratio on compressibility effects in rectangular microchannels is disregarded in the open literature but it can be very important for the design of microdevices. This paper aims to fill this gap investigating numerically and experimentally the role played by compressibility in rectangular microchannels. The goal is to calculate, for a fixed aspect ratio, the Reynolds number in correspondence of which the compressibility of the working fluid cannot be ignored for the accurate estimation of the friction factor. This problem is crucial for the design of micro heat exchangers and micro heat sinks in which gas flows are used as working fluids.

2. Mathematical model

In the present investigation the behaviour of a gas flow through a microchannel featuring a rectangular cross-section, with aspect ratio $\beta \leq 1$ defined as the ratio of the width (w) to the height (h) of the microchannel, is studied numerically. To investigate the dynamic behaviour of the flow, the reducer connecting the entrance manifold to the supply piping and the reducer connecting the exit manifold to the ambient are also considered, as shown in Fig. 1.

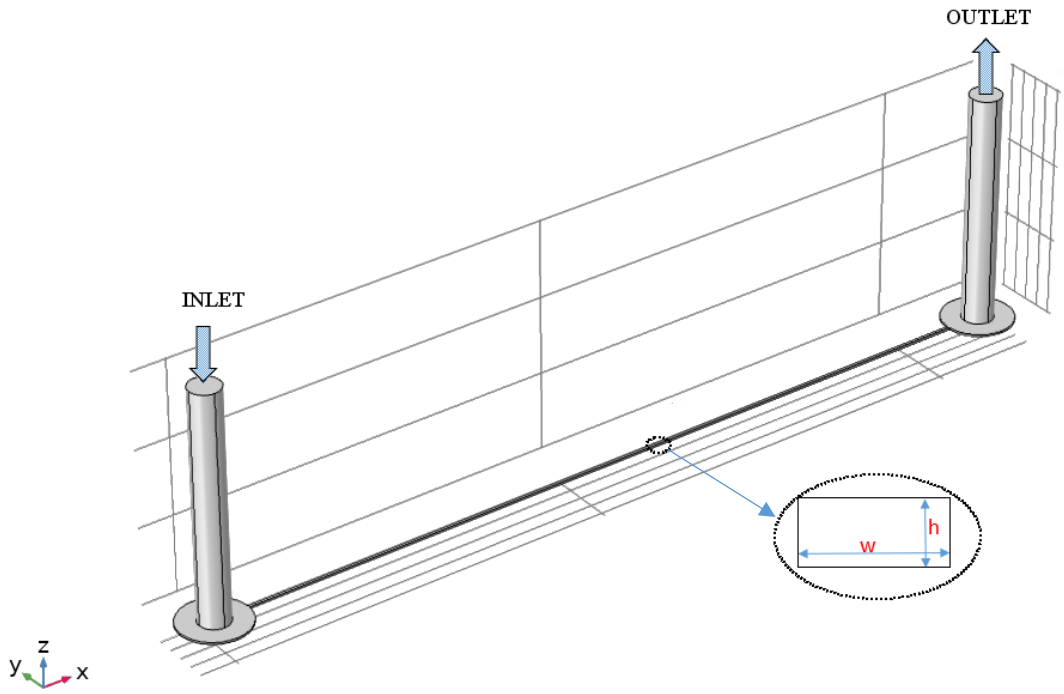

Figure 1. Geometry under investigation.

By assuming that all the transport processes are in a steady state, the gas is a Newtonian fluid with constant properties with the exception of the dynamic viscosity, no free convection, chemical reactions, electromagnetic effects and mass diffusion, rigid channel walls, the complete set of the governing balance equations were the as follows:

$$\nabla \cdot \boldsymbol{v} = 0 \tag{1}$$

$$\rho \frac{D\boldsymbol{v}}{Dt} = -\nabla p + (\nabla \cdot \boldsymbol{\tau})$$

$$\rho \frac{DH}{Dt} = -(\nabla \cdot \boldsymbol{q}) + (\boldsymbol{\tau} : \nabla \boldsymbol{v}) + \frac{Dp}{Dt}$$

coupled with the constitutive laws for an ideal gas:

$$\rho = \frac{p}{RT}; H = c_p T \tag{2}$$

where $\boldsymbol{v}$ indicated the velocity field, ρ the fluid density, t the time, p the pressure, $\boldsymbol{\tau}$ the stress tensor, H the gas enthalpy, q the heat flow, R was the universal gas constant, T the fluid temperature and c_p the specific heat at constant pressure.
In the energy balance equation, the first term of the r.h.s. was the diffusive heat flux, the second term represented the viscous dissipation term and the third term was the flow work.
The balance equations were solved by considering the following boundary conditions: i) inlet section: static pressure and temperature; ii) outlet section: pressure; iii) walls: adiabatic and no slip boundary condition.
Dynamic viscosity dependence on gas temperature was defined using Sutherland's law:

$$\mu = \mu_{ref} \left(\frac{T}{T_{ref}} \right)^{\frac{3}{2}} \left(\frac{T_{ref} + S_h}{T + S_h} \right) \tag{3}$$

where T_{ref} was the reference temperature, μ_{ref} the viscosity at the reference emperature and S_h the Sutherland temperature.
For the purpose of the present study, the Reynolds and the Mach numbers were also evaluated. The average value of the Reynolds number was calculated as follows:

$$Re = \frac{\bar{\rho} \bar{v} D_h}{\bar{\mu}} \tag{4}$$

where $\bar{\rho}$, $\bar{v}$ and $\bar{\mu}$ were the average density, velocity and dynamic viscosity of the gas at a cross-section, respectively, and D_h the hydraulic diameter of the channel, which was defined as:

$$D_h = \frac{4A}{P} \tag{5}$$

where A and P were average cross sectional area and wetted perimeter, respectively.
For compressible flows the Reynolds number could change between inlet and outlet of the tube due to the flow acceleration along the axial direction. For isothermal flows the Reynolds number defined by Eq.(4) is constant along the microtube [6].
The average value assumed by Mach number was evaluated by:

$$Ma = \frac{\bar{v}}{\sqrt{\gamma R_s \bar{\bar{T}}}} \tag{6}$$

Finally, the average friction factor was evaluated. By assuming that the flow was one-dimensional flow, the mean friction factor between two relatively distant points across the channel could be expressed as follows [22]:

$$f_f = \frac{D_h}{x_2 - x_1}\left[-2ln\left(\frac{p_1}{p_2}\right) + 2ln\left(\frac{T_1}{T_2}\right) - \frac{1}{\left[\rho_{in}^2 u_{in}^2 R_s\left(T_{in} + \frac{u_{in}^2}{2c_p}\right)\right]}\left\{\frac{p_2^2 - p_1^2}{2} + \frac{B^2}{2} ln\left(\frac{p_2 + \sqrt{p_2^2 + B^2}}{p_1 + \sqrt{p_1^2 + B^2}}\right) + \frac{1}{2}\left(p_2\sqrt{p_2^2 + B^2} - p_1\sqrt{p_1^2 + B^2}\right)\right\}\right] \quad (7)$$

being R_s the specific gas constant, x the axial location and $\dot{G}$ the mass flow rate per unit area. The subscripts *1* and *2* referred to the different locations across the channel.
B^2 was defined as follows:

$$B^2 = 4\alpha\frac{\rho_{in}^2 u_{in}^2 {R_s}^2}{2c_p}\left(T_{in} + \frac{u_{in}^2}{2c_p}\right) \quad (8)$$

By means of Eq.(7) it is possible to evaluate the average friction factor between two locations that are not close such as the inlet and the outlet.

3. Mesh independence analysis

To get mesh-independent results, different grid sizes were tested. For each grid, characterized by hexahedral cells, the average friction factor evaluated by means of Eq. (7) was monitored. The geometrical properties of the investigated microchannel, manifolds and reducers are summarized in Table 1. These geometrical characteristics were chosen because the numerical model adopted in the present study was validated against the experimental data that were obtained using this kind of microchannel [18]. For the same reason, Nitrogen was considered as working fluid (constants for Nitrogen gas were as follows: μ_{ref} = 1.7812·10^{-5} Pa·s, T_{ref} = 298.15K and S_h = 111 K).
The governing equations with the linked boundary conditions were solved using the commercial software Comsol Multiphysics© 5.6, resorting to the parallel sparse direct linear solver PARDISO [23].

Table 1: Geometrical data of microchannel, manifolds and reducers.

Inlet reducer diameter [μm]	400
Inlet reducer height [μm]	3000
Inlet manifold diameter [μm]	900
Microchannel height [μm]	250
Microchannel width [μm]	360
Outlet manifold diameter [μm]	900
Outlet reducer diameter [μm]	400
Outlet reducer height [μm]	3000

The results of the grid convergence study are presented in figure 2 for some representative cases investigated in the present study. It can be observed that for $\beta = 0.25$ and for $D_h = 100$ μm and $D_h = 295$ μm, mesh independent results can be obtained for a number of finite elements (N) higher than $2 \cdot 10^5$. The analysis of the results obtained for the other values of the aspect ratio and for $D_h = 500$ μm leads to the same conclusion. Therefore, all the results presented in the next sections were obtained by adopting a grid characterized by at least $2 \cdot 10^5$ elements.

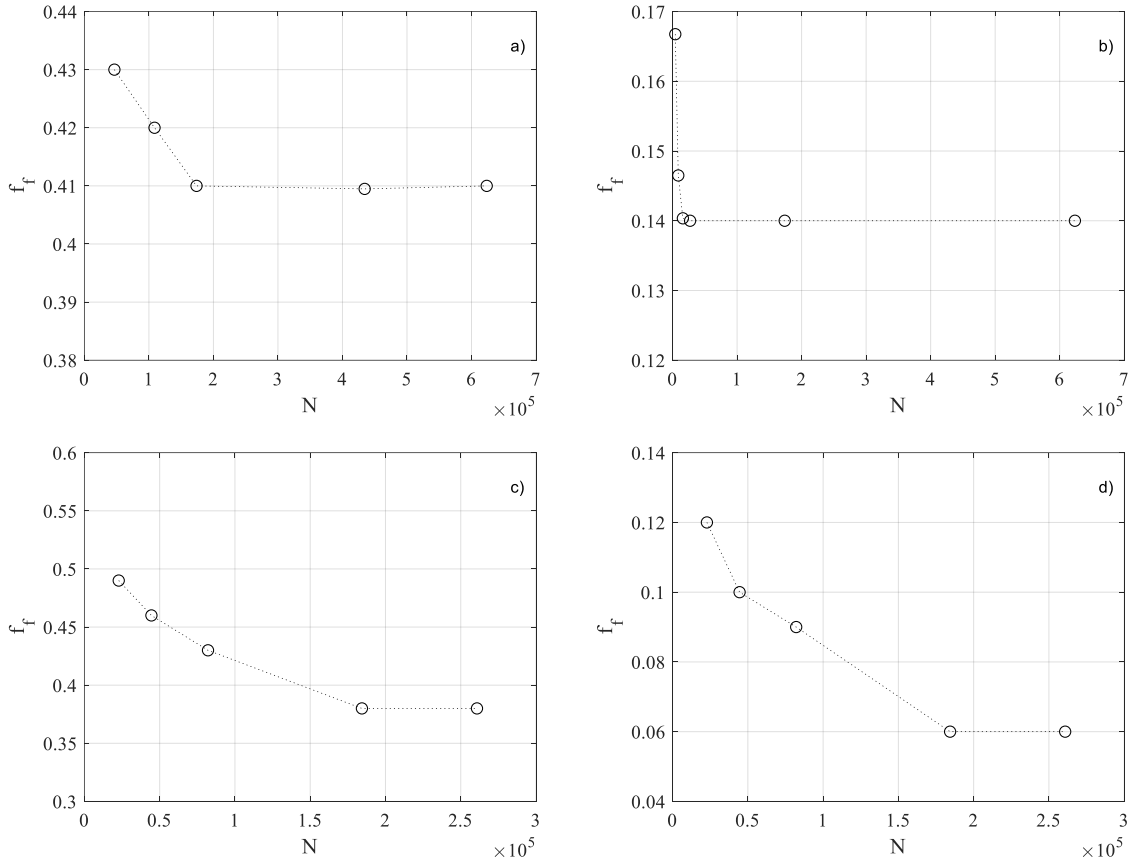

Figure 2. Average friction factor as a function of the element number for $\beta = 0.25$. $D_h = 100$ μm and $Re = 200$; b) $D_h = 100$ μm and $Re = 600$; c) $D_h = 295$ μm and Re=200; d) $D_h = 295$ μm and $Re = 1400$.

4. Experimental validation

The accuracy of the results obtained by adopting the numerical model adopted in the present study were assessed by comparing the numerical results with the experimental data available in literature. In the interests of clarity, in the present paragraph some details about the experimental set-up and procedure are reported. Detailed information can be found in [18].

The experimental tests were carried out for a wide range of Reynolds number (i.e. $200 \leq Re \leq 1800$) in isothermal flow conditions. Nitrogen was used as working fluid, as shown in figure 3 where a picture of the experimental set up is presented. The width and the height of the investigated microchannel were 360 μm and 250 μm, respectively. Therefore, the aspect ratio, the hydraulic diameter and the length of the investigated microchannel were $\beta = 0.69$, $D_h = 295$ μm and $L = 100$ mm, respectively.

The average friction factor was evaluated by applying Eq.(7) between the inlet and the outlet sections of the microchannel; the uncertainty in evaluating f_f, which was estimated by applying the error propagation theory, was about ±10%.

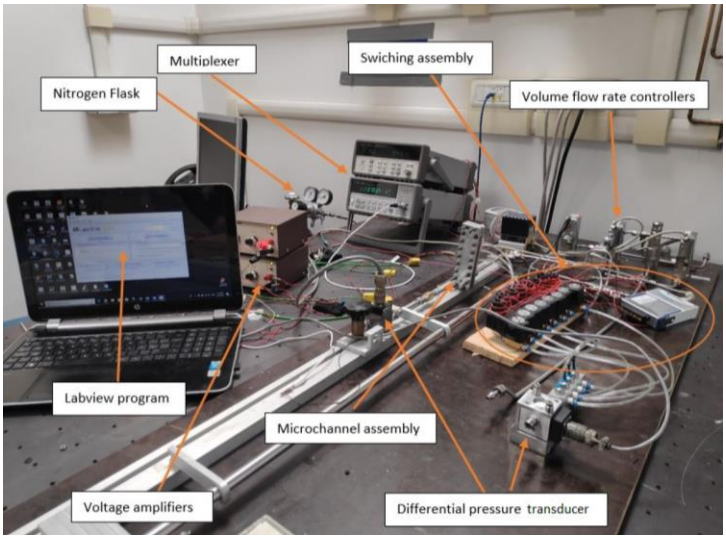

Figure 3. Experimental set up [18].

The experimental values of the average friction factor were used to assess the accuracy of the numerical results, as shown in figure 4 where the numerical values of the average friction factors are compared to experimental data.

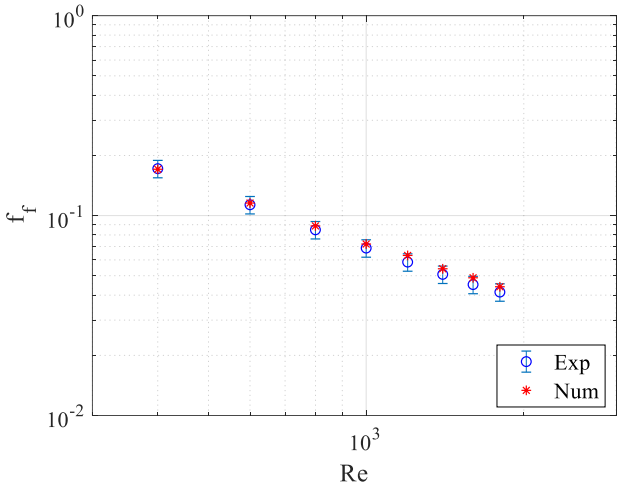

Figure 4. Comparison between numerical and experimental data.

The comparison reveals that the numerical values of f_f are within the uncertainty associated to the experimental values, thus confirming that the numerical tool allows evaluating the average friction factor with a satisfactory accuracy.

5. Results

The numerical model validated against experimental data was adopted to evaluate the influence of the compressibility on the average friction factor. The computations were performed for a wide range of Reynolds number and for isothermal flow conditions by considering nitrogen as working fluid. The influence of the compressibility on the average friction factor for the channel experimentally investigated (i.e. $\beta = 0.69$, D_h = 295 μm and L = 100 mm) is presented in figure 5 where the average Poiseuille number ($f_f \cdot Re$), defined as the product between the average friction factor and the Reynolds

number at the inlet of the channel, is depicted as a function of the Mach number. Here the Mach number is the average between the inlet and the outlet of the microchannel [12]:

$$Ma = \frac{(Ma_{in} + Ma_{out})}{2} \tag{9}$$

The Poiseuille number is not a function of Mach for incompressible flows. In figure 5 the Poiseuille number for incompressible flows is calculated by using the Shah and London correlation [24] for laminar flows in rectangular channels.

It has to be pointed out that due to compressibility effects the value of the Reynolds number changes along the microchannel length, therefore different values of *Re* can be adopted. Since in the experiments it is easier to evaluate the Reynolds number at the inlet section of the channels, all the data presented in the next figures were obtained by considering *Re* at the inlet of the channel.

By comparing the numerical values of the average friction factor with the corresponding values evaluated by Shah and London [24] a positive deviation from the conventional incompressible flow theory was observed for *Re* higher than 400. The numerical values of the Poiseuille number are obtained by considering the average friction factor along the whole channel, therefore the difference between the numerical values and those predicted from the Poiseuille law is due to the entrance effects, gas compressibility effects and to the density variation (i.e. the values reported in [24] were evaluated in the fully-developed region, but for compressible flow the velocity profile always changes in axial direction). Observing Figure 5, the Poiseuille number, which is constant in laminar regime for incompressible flows, evidences an increase when the Mach number increases. Even for low values of the Mach number ($Ma < 0.2$ which corresponds to $Re < 1400$) an evident deviation from the incompressible Poiseuille number (dashed line in Figure 5) is observed; as expected, the deviation increases by increasing the Mach number.

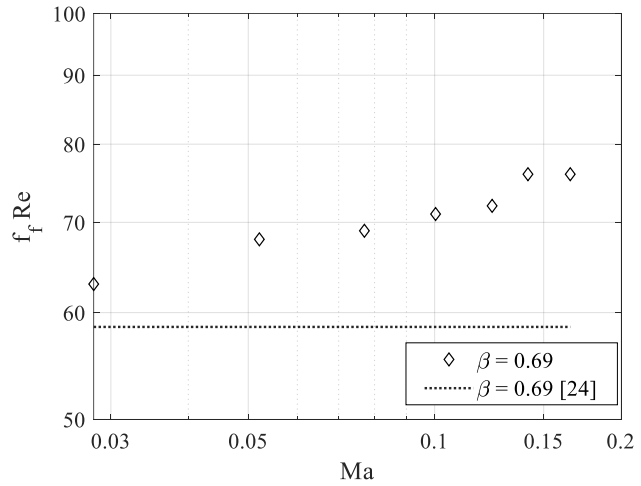

Figure 5. $f_f \cdot Re$ as a function of the Mach number for $\beta = 0.69$, $L = 100$ mm and $D_h = 295$ μm.

To evaluate the influence of the aspect ratio, other four values of β were considered, namely $\beta = 0.25$, $\beta = 0.50$, $\beta = 0.75$ and $\beta = 1$, keeping the same values of the hydraulic diameter and channel length. The comparison between the numerical values of the average friction factor and the theoretical predictions for incompressible flows [24] is presented in figure 6 for all the values of the aspect ratio considered in the present study. It was observed an increase of the friction factor with respect to the conventional incompressible flow theory even for the other values of the aspect ratio, although the value of the Reynolds number at which the deviation started was dependent on β.

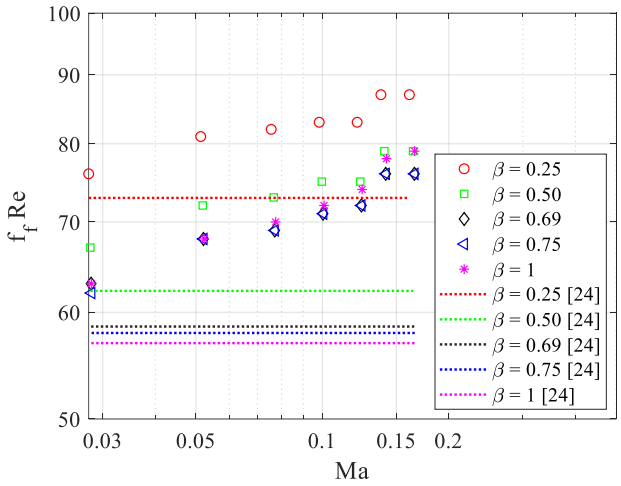

Figure 6. f_f·*Re* as a function of the Mach number for D_h = 295 μm and L = 100 mm.

To quantify the increase in the average friction factor of the compressible flow with respect to the incompressible flow, the relative error between the friction factor for compressible flows and the friction factor for incompressible flows was evaluated as follows:

$$\Delta_{f_f} = \frac{f_{f,comp} - f_{f,incomp}}{f_{f,incomp}} \tag{10}$$

The values of the relative error Δ_{f_f} evaluated by means of Eq.(10), for D_h = 295 μm and for all values of the aspect ratio considered in the present study are reported in Table 2.
In figure 7 the axial trend of the local Poiseuille number is shown as a function of the distance from the inlet section (x) for a rectangular channel having β = 0.69, D_h = 295 μm and L = 100 mm is presented. The Reynolds number at the inlet is equal to 1400.

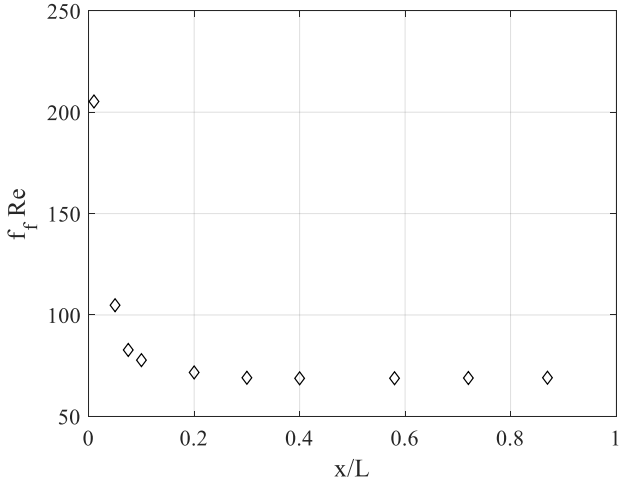

Figure 7. f_f·*Re* as a function of axial coordinate for β = *0.69*, D_h = 295 μm, L = 100 mm and *Re* = 1400.

It is evident that the entrance effects tend to become negligible for x/L >0.2 and the Poiseuille number tends to become constant. To highlight the influence of the only compressibility effects on the friction factor, the numerical values of the relative error Δ_{f_f} were then evaluated by excluding the entrance region in the average calculation of the friction factor.
The values obtained excluding the entrance region are reported in Table 2 for a direct comparison with the data obtained considering the entrance region.
By observing the data reported in Table 2 it can be deduced that, as expected, the increase in the friction factor is higher for high values of the Reynolds number, since flow accelerates with the increase in *Ma* and *Re*. Moreover, it can be observed that the value of the relative error between the friction factor for compressible flows and the friction factor for incompressible flows evaluated by means of Eq.(10) increases as the aspect ratio increases. This finding can be explained by considering that in correspondence of low values of β the acceleration due to the compressibility effects is hampered by the deceleration caused by the increase in the cross-sectional area.
In Table 2 the relative error Δ_{f_f} (Eq.(10)) is reported as a function of the channel aspect ratio and Reynolds number. The highest difference between the average friction factor for compressible flows and the corresponding one for incompressible flows was 31% at *Re* =1400 for a squared microchannel with D_h=295 mm, thus confirming that the compressibility effects play a leading role in the evaluation of the friction factor in rectangular microchannels. However, ignoring the entrance effects, an increase of 23% of the average friction factor is obtained by considering only compressibility effects.
By observing the data reported in Table 2 it is evident how, for narrow microchannels, compressibility effects become more evident for large Reynolds numbers, while for squared microchannels they are important even at low *Re*.

Table 2: Relative error between the friction factor for compressible flows and the friction factor for incompressible flows Δ_{f_f} (D_h = 295 μm) with (in bold) or without entrance effects.

	Re						
β	200	400	600	800	1000	1200	1400
0.25	**4-**4%	**5-**5%	**7-**7%	**8-**8%	**10-**9%	**11-**9%	**13-**11%
0.5	**7-** 7%	**9-**9%	**12-**11%	**14-**12%	**16-**14%	**18-**15%	**21-**17%
0.69	**7-**7%	**10-**10%	**13-**12%	**15-**13%	**18-**15%	**20-**16%	**23-**18%
0.75	**8-**7%	**11-**10%	**14-**12%	**16-**14%	**19-**15%	**21-**17%	**24-**18%
1	**8-**8%	**13-**13%	**17-**15%	**20-**17%	**24-**19%	**27-**21%	**31-**23%

Compressibility effects play an important role although the average Mach number, evaluated by means of Eq.(9), is lower than 0.3 (i.e. for D_h = 295 μm *Ma* ranges between 0.03 and 0.17 in correspondence of the conditions considered in Table 2). In fact, as discussed by Morini et al. [7] when the ratio of the net pressure drop to the inlet pressure is higher than 0.05, although the gas flow can be locally modeled as incompressible, the density variation along the tube cannot be disregarded. Therefore, the effects due to the gas acceleration along the tube become important, even if the Mach number is low.
To better evaluate the influence of the microchannel hydraulic diameter, other two representative values of D_h, namely D_h = 100 μm and D_h = 500 μm were considered. The same trends were observed even for these two values of the hydraulic diameter. In figure 8, the comparison between the numerical values of the average friction factor and the theoretical predictions for incompressible flows [24], for D_h = 100 μm, $0.25 \leq \beta \leq 1$ and for $200 \leq Re \leq 600$ is shown. For these operating conditions, the average Mach number ranges between 0.06 and 0.17.
It can be observed that for this low value of the hydraulic diameter the deviation of the average friction factor from the predicted one for incompressible flows becomes evident at lower Reynolds numbers, as

also highlighted by other researchers who investigated compressibility effects in different geometries [8,10].

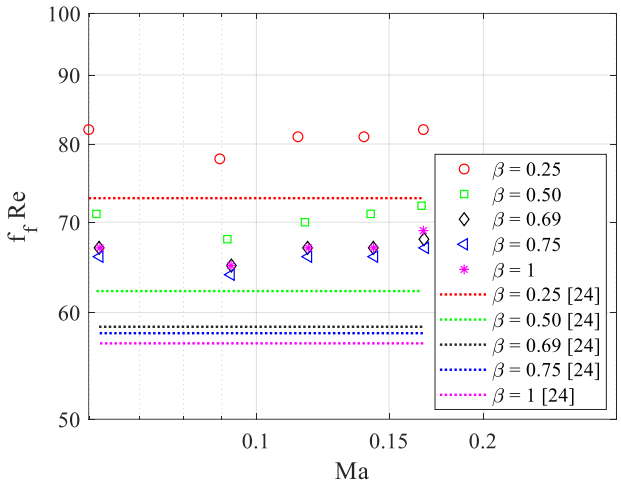

Figure 8. f_f·*Re* as a function of the Mach number for D_h = 100 μm and *L*=100 mm.

The values of the relative error between the friction factor for compressible flows and the friction factor for incompressible flows Δ_{f_f} evaluated by means of Eq.(10), for D_h = 100 μm are reported in Table 3 with and without to take into account entrance effects. It can be observed that the highest difference between the average friction factor for compressible flows and the predictions for incompressible flows is 20% and it occurs for *Re* = 600, thus highlighting the importance of compressibility effects in microchannels characterized by small hydraulic diameters. It has to be highlighted that since the purpose of the analysis was to evaluate the value of the Reynolds number at which compressibility effects became significant, for D_h = 100 μm the analysis was limited to $200 \leq Re \leq 600$.
From the data reported in Table 3, it can be deduced that the entrance effects are not significant in the evaluation of the friction factor in very small microchannels, since the values of the relative error between the friction factor for compressible flows and the friction factor for incompressible flows with or without entrance effects are the same. This finding underlines that, due to the fact that the entrance effects are strongly reduced at low values of the Reynolds number, compressibility effects becomes predominant in smaller microchannels where compressibility is significant even at low *Re*.

Table 3: Relative error between the friction factor for compressible flows and the friction factor for incompressible flows Δ_{f_f} (D_h= 100 μm) with (in bold) or without entrance effects.

	Re				
β	200	300	400	500	600
0.25	**8**-8%	**9**-9%	**11**-11%	**12**-12%	**13**-13%
0.5	**10**-10%	**12**-12%	**13**-13%	**14**-14%	**15**-15%
0.69	**10**-10%	**13**-13%	**13**-13%	**15**-15%	**16**-16%
0.75	**10**-10%	**12**-12%	**13**-13%	**15**-15%	**16**-16%
1	**13**-13%	**15**-15%	**17**-17%	**19**-19%	**20**-20%

To explain the results reported in Table 3 one has to bear in mind that the Poiseuille number is a function of the aspect ratio for rectangular channels: the shallow cross section exhibits larger Poiseuille numbers

(which means a larger friction factor for a constant Reynolds number). This means that for shallow microchannels, larger pressure drop values are expected if compared with the squared ones at the same Reynolds numbers and the same hydraulic diameter. Larger pressure drop values justify a more evident compressible behaviour of the gas if compared with squared channels. By observing the definition of Δ_{f_f} (Eq.10), both denominator (friction factor) and numerator (compressibility effect) increase when the channel aspect ratio is reduced but the increase of denominator is larger than numerator. This fact explains the counter intuitive trend of Δ_{f_f} reported in Table 3: shallow microchannels are characterized by larger compressibility effects and pressure drop but, as percentage, the increase of the friction factor due to compressibility effect is smaller than the increase of pressure drop due to the cross section geometry.

On the contrary, as the hydraulic diameter increases compressibility effects become less important, as confirmed by the numerical outcomes obtained for D_h = 500 μm.

In particular, it was observed that for this value of the hydraulic diameter the deviation of the average friction factor from the predicted one for incompressible flows started for high values of the Reynolds number, as shown in figure 9, where the comparison between the numerical values of the average friction factor and the theoretical predictions for incompressible flows [24] for D_h = 500 μm, $0.25 \leq \beta \leq 1$ and for $200 \leq Re \leq 1200$, is presented. For these operating conditions, the average Mach number ranges between 0.02 and 0.1.

The relative error between the friction factor for compressible flows and the friction factor for incompressible flows Δ_{f_f} evaluated by means of Eq.(10) is reported in Table 4.

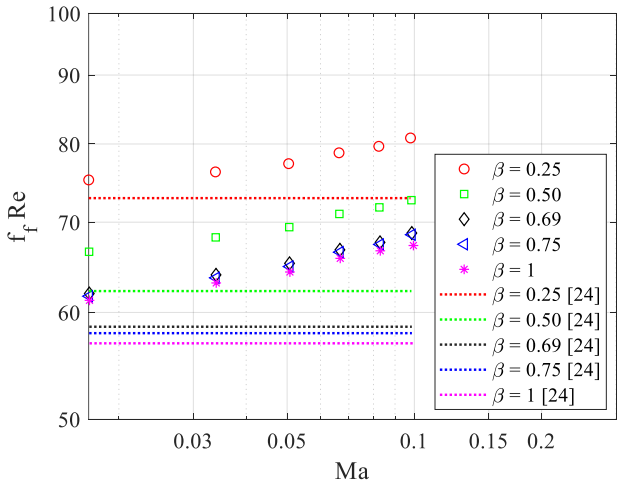

Figure 9. f_f·Re as a function of the Mach number for D_h= 500 μm and L=100 mm.

By focusing the attention on the compressibility effects on the friction factor (see Table 4), it was found that for the highest values of the Reynolds number and aspect ratio considered in the present study, the maximum discrepancy between the numerical values of the average friction factor and the predicted ones for incompressible flows was 13%, thus confirming that for high values of the hydraulic diameter the gas compressibility becomes important only for high values of the Reynolds number. It is also evident that entrance effects on the average friction factor are stronger in larger microchannels.

Table 4: Relative error between the friction factor for compressible flows and the friction factor for incompressible flows Δ_{f_f} (D_h = 500 μm) with (in bold) or without entrance effects.

Re

β	200	400	600	800	1000	1200
0.25	**3**-3%	**5**-5%	**7**-6%	**8**-7%	**10**-8%	**11**-8%
0.5	**7**-7%	**10**-9%	**12**-10%	**14**-11%	**16**-12%	**17**-13%
0.69	**6**-5%	**10**-8%	**12**-9%	**14**-11%	**16**-12%	**17**-13%
0.75	**6**-5%	**10**-8%	**13**-10%	**15**-11%	**17**-12%	**18**-13%
1	**8**-6%	**11**-9%	**14**-10%	**16**-11%	**17**-12%	**19**-13%

The numerical outcomes were processed to develop correlations that enable to account for compressibility and entrance effects in the evaluation of the friction factor. To this aim, the increase in the friction factor Ψ was evaluated by comparing the product $f_f \cdot Re$ for compressible flows with the corresponding value for incompressible flow [24]:

$$\Psi = \frac{f_{f,comp} \cdot Re}{f_{f,incomp} \cdot Re} \tag{11}$$

The correction factor Ψ can be calculated by using the following correlation generated with the numerical data shown previously:

$$\Psi = 0.87 + 0.75 \cdot \beta + 2.25 \cdot Ma - 1.09 \cdot \beta^2 - 0.86 \cdot \beta \cdot Ma - 17.08 \cdot Ma^2 + 0.51 \cdot \beta^3 + 1.29 \cdot \beta^2 \cdot Ma - 2.99 \cdot \beta \cdot Ma^2 + 60.02 \cdot Ma^3 \tag{12}$$

This correlation is valid for rectangular microchannels with $100 \leq D_h \leq 500$ μm and $0.25 \leq \beta \leq 1$, in the range of Reynolds number 200-600.
On the contrary, for rectangular microchannels with $295 \leq D_h \leq 500$ μm and $0.25 \leq \beta \leq 1$, in the range of Reynolds number 600-1200, Ψ can be evaluated by means of the following correlation:

$$\Psi = 0.83 + 1.07 \cdot \beta + 1.8 \cdot Ma - 1.49 \cdot \beta^2 - 1.7 \cdot \beta \cdot Ma - 10.9 \cdot Ma^2 + 0.65 \cdot \beta^3 + 1.6 \cdot \beta^2 \cdot Ma - 4.86 \cdot \beta \cdot Ma^2 + 30.06 \cdot Ma^3 \tag{13}$$

The maximum error between the numerical values of the average friction factor and the values obtained by applying the above correlations is lower than 2% with a standard deviation lower than 1%. The comparison between numerical and estimated average friction factors is presented in figure 10. In the same figure, the confidence intervals are also reported. They are evaluated by considering the standard deviation of the estimation errors on the friction factor.
The numerical values of the average friction factor are also compared with the results obtained by applying previous the correlations proposed by Hong et al. [17]. The maximum discrepancy is about 13% and it occurs for $D_h = 100$ μm, $\beta = 1$ and $Re = 400$. This difference is mainly due to the very low values of the aspect ratio investigated in [17] (i.e. $\beta \leq 0.1$) which can be considered a limit for the correlations proposed by Hong et al.
However, the correlations proposed in this paper are in an overall agreement with the previous works, and enable to extend the prediction of f_f for high values of both aspect ratio and Reynolds number.

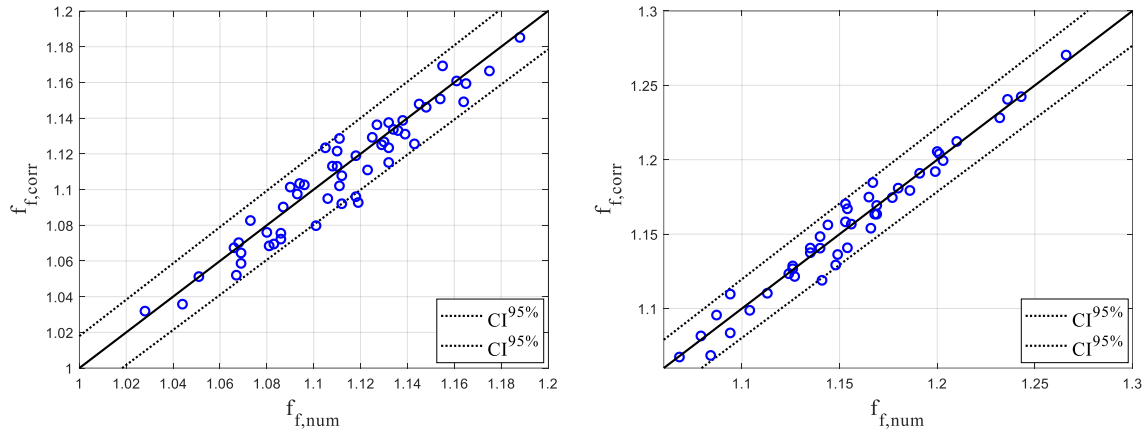

Figure 10. Comparison between numerical and estimated average friction factor. a) $100 \leq D_h \leq 500$ μm and $200 \leq Re < 600$; b) $295 \leq D_h \leq 500$ μm and $600 \leq Re \leq 1200$.

6. Conclusions

In this paper a numerical evaluation of the influence of gas compressibility on the average friction factor in rectangular microchannels is presented. The governing balance equations were solved by using Comsol Multiphysics and by considering nitrogen as working fluid in laminar regime. Experimental data available in literature were used to validate the numerical model.
The main conclusions of this analysis can be summarized as follows:

- compressibility effects lead to an increases in the average friction factor; the difference between the theoretical predictions for incompressible flows and the corresponding values for compressible flows depends on the values of the aspect ratio and hydraulic diameter;
- for narrow microchannels (low aspect ratio β) compressibility effects become important for high values of the Reynolds number, while for squared microchannels ($\beta \rightarrow 1$) they are important even for low values of Re;
- compressibility effects are very important in microchannels characterized by small hydraulic diameters by evidencing their effects at low Reynolds numbers.
- in comparison to incompressible flows, for D_h=500 μm, the compressibility effects increase the average friction factor up to 13% at Re=1200; for D_h=295 μm the increase becomes equal to 23% at the same Reynolds number (Re=1200). For a smaller rectangular channel (D_h=100 μm) the increase is larger by reaching 20% at Re=600.

Nomenclature

A	Average cross sectional area
c_p	Specific heat at constant pressure
D_h	Hydraulic diameter of the channel
f	Fanning friction factor

$f_f Re$	Poiseuille number
$\dot{G}$	Mass flow rate per unit area
h	Height of the microchannel
H	Gas enthalpy
k	Fluid thermal conductivity
P	Wetted perimeter
p	Fluid pressure
Ma	Mach number
Re	Reynolds number
R	Universal gas constant
R_s	Specific gas constant
q	Heat flux
t	Time
T	Fluid temperature
$\boldsymbol{v}$	Velocity vector
$\bar{v}$	Average fluid velocity
w	Width of the microchannel
x,y,z	Cartesian coordinates
Greek symbols	
β	Aspect ratio
μ	Fluid dynamic viscosity
ρ	Fluid density
τ	Stress tensor

References

[1] Morini G.L., Yang Y., 2013. Guidelines for the analysis of single-phase forced convection in microchannels. ASME Journal of Heat Transfer 135, 101004. https://doi.org/10.1115/1.4024499

[2] Guo Z., Wu X. 1997. Compressibility effect on the gas flow and heat transfer in a microtube. International Journal of Heat and Mass Transfer 40(13), 3251-3254. https://doi.org/10.1016/S0017-9310(96)00323-7

[3] Guo Z.Y., Wu X.B. 1998. Further study on compressibility effects on the gas flow and heat transfer in a microtube. Microscale Thermophysical Engineering 2(2), 111-120. https://doi.org/10.1080/108939598200024

[4] Guo Z-Y., Li, Z-X. 2003. Size effect on microscale single-phase flow and heat transfer. International Journal of Heat and Mass Transfer 46(1), 149-159. https://doi.org/10.1016/S0017-9310(02)00209-0

[5] Morini G.L., Lorenzini M., Salvigni S. 2006. Friction characteristics of compressible gas flows in microtubes," Experimental Thermal and Fluid Science, vol. 30(8), 733-744. https://doi.org/10.1016/j.expthermflusci.2006.03.003
[6] Shapiro A. H. *The Dynamics and Thermodynamics of Compressible Fluid Flow*, vol. 1. John Wiley & Sons, Inc: New Jersey, 1953.
[7] Morini G.L., Lorenzini M, Colin S., Geoffroy S. 2007. Experimental analysis of pressure drop and laminar to turbulent transition for gas floes in smooth microtubes. Heat Transfer Eng. 28 (8–9), 670–679. https://doi.org/10.1080/01457630701326308
[8] Celata G., Cumo M., McPhail S., Tesfagabir L., Zummo G. 2007. Experimental study on compressible flow in microtubes. International Journal of Heat and Fluid Flow 28(1), 28-36. https://doi.org/10.1016/j.ijheatfluidflow.2006.04.009
[9] Celata G., Lorenzini M., Morini G.L. 2009. Friction factor in micropipe gas flow under laminar, transition and turbulent flow regime. Int J Heat Fluid Flow 30, 814-822. https://doi.org/10.1016/j.ijheatfluidflow.2009.02.015
[10] Tang, G.H., Li, Z., He, Y.L., Tao, W.Q. 2007. Experimental study of compressibility, roughness and rarefaction influences on microchannel flow. International Journal of Heat and Mass Transfer 50(11-12), 2282-2295. 10.1016/j.ijheatmasstransfer.2006.10.034
[11] Vijayalakshmi, K., Anoop, K.B., Patel, H.E., (...), Sundararajan, T., Das, S.K. 2009. Effects of compressibility and transition to turbulence on flow through microchannels. International Journal of Heat and Mass Transfer 52(9-10), 2196-2204. https://doi.org/10.1016/j.ijheatmasstransfer.2008.07.056
[12] Hong, C., Asako, Y., Faghri, M., Morini, G.L. 2020. Average friction factor for laminar gas flow in microtubes. CFD Letter 12(3), 22-30. https://doi.org/10.37934/cfdl.12.3.2230
[13] Wu P., Little W. 1983. Measurement of friction factors for the flow of gases in very fine channels used for microminiature Joule-Thomson refrigerators. Cryogenics. 23(5), 273-277. https://doi.org/10.1016/0011-2275(83)90150-9
[14] Asako Y., Pi T., Turner S.E., Faghri M. 2003. Effect of compressibility on gaseous flows in micro-channels. International Journal of Heat and Mass Transfer 46 (16), 3041-3050. https://doi.org/10.1016/S0017-9310(03)00074-7
[15] Hong C., Asako Y., Lee J.H. 2008. Poiseuille number correlation for high speed microflows. J. Phy. D Apll. Phy., 41, 10. https://doi.org/10.1088/0022-3727/41/10/105111
[16] Cavazzuti, M., Corticelli, M.A., Karayiannis, T.G. 2019. Compressible Fanno flows in micro-channels: An enhanced quasi-2D numerical model for laminar flows. Thermal Science and Engineering Progress 10, 10-26. https://doi.org/10.1016/j.tsep.2019.01.003
[17] Hong C., Yamada T., Asako Y., Faghri M. 2012. Experimental investigation of laminar, transitional and turbulent gas flow in microchannels. International Journal of Heat and Mass Transfer 55, 4397-4403. https://doi.org/10.1016/j.ijheatmasstransfer.2012.04.008
[18] Rehman, D., Morini, G.L., Hong, C. 2019. A comparison of data reduction methods for average friction factor calculation of adiabatic gas flows in microchannels. Micromachines 10(3), 171. https://doi.org/10.3390/mi10030171
[19] Morini G.L., Brandner J. The Design of Mini/Micro Heat Exchangers: A World of Opportunities and constraints, IHTC16-KN29, *Proc. of the 16th International Heat Transfer Conference*, *IHTC-16*, August 10-15, 2018, Beijing, China
[20] Morini, G.L., Laminar Liquid Flow Through Silicon Microchannels. 2004. ASME Journal of Fluids Engineering 126(3), 485-489. https://doi.org/10.1115/1.1760545
[21] Ahmed H.E., Salman B.H., Kherbeet A.S., Ahmed M.I. 2018. Optimization of thermal design of heat sinks: a review. International Journal of Heat and Mass Transfer 118, 129-153. https://doi.org/10.1016/j.ijheatmasstransfer.2017.10.099
[22] Hong, C., Asako, Y., Morini, G.L., Rehman, D. 2019. Data reduction of average friction factor of gas flow through adiabatic micro-channels. International Journal of Heat and Mass Transfer 129, 427-431. https://doi.org/10.1016/j.ijheatmasstransfer.2018.09.088
[23] Schenk, O., Gärtner, K., Fichtner, W., Stricker, A. 2001. PARDISO: A high-performance serial

and parallel sparse linear solver in semiconductor device simulation. Future Generation Computer Systems 18(1), 69-78. https://doi.org/ 10.1016/S0167-739X(00)00076-5
[24] Shah R.K., London A.L. *Laminar Flow Forced Convection in Ducts.* Academic Press: New York, 1978.